Accepted Manuscript

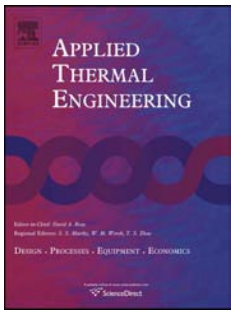

Experimental investigation of thermal balance of a turbocharged SI engine operating on natural gas

A. Gharehghani, M.Koochak, M. Mirsalim, Talal Yusaf

PII: S1359-4311(13)00454-7

DOI: 10.1016/j.applthermaleng.2013.06.029

Reference: ATE 4880

To appear in: *Applied Thermal Engineering*

Received Date: 11 February 2013

Accepted Date: 13 June 2013

Please cite this article as: A. Gharehghani, M.Koochak, M. Mirsalim, T. Yusaf, Experimental investigation of thermal balance of a turbocharged SI engine operating on natural gas, *Applied Thermal Engineering* (2013), doi: 10.1016/j.applthermaleng.2013.06.029.

Experimental investigation of thermal balance of a turbocharged SI engine operating on natural gas

A. Gharehghani[*a], M.Koochak[b], M. Mirsalim[a], Talal Yusaf[c]

[a] Department of Mechanical Engineering, Amirkabir University of Technology, 424 Hafez Avenue, P.O. Box 15875-4413, Tehran, Iran

[b] Department of Mechanical Engineering, K. N. Toosi University of Technology, Iran

[c] Faculty of Engineering and Surveying, University of Southern Queensland, Toowoomba, 4350 QLD, Australia

Abstract

This paper experimentally investigates the thermal balance and performance of a turbocharged gas spark ignition engine. The First Law of Thermodynamics was used for control volume around the engine to compute the output power, transferred energy to the cooling fluid, exhaust gases and also unaccounted losses through convection and radiation heat transfer. Thermal balance tests were performed for various operational conditions including full and half loads and different cooling fluid temperatures. Results indicate that by increasing engine load and coolant temperature, the percentage of transferred energy to the exhaust gases increased while the percentage of coolant energy decreased. Also, experimental data reveals that using gaseous fuel and a turbocharger (TC) in the engine leads to 4.5% and 4% more thermal efficiency than gasoline and natural aspirated (NA), respectively. Also, second law analysis reveals that using a turbocharger leads to a 3.6% increase in exergetic efficiency of the engine, averagely. Based on experimental results, an empirical correlation was suggested for computing the energy of exhaust gases which shows good agreement with the experimental data for the majority of operating conditions.

Keywords: Thermal balance, Gas SI engine, Energy of exhaust gas, Turbocharger, Exergetic efficiency

[*] **Corresponding Author:** Department of Mechanical Engineering, Amirkabir University of Technology, 424 Hafez Avenue, P.O. Box 15875-4413, Tehran, Iran, ayatallah@aut.ac.ir

1. Introduction

Energy is supplied to the engine as the chemical energy of the fuel and leaves as output power, energy transferred to cooling fluid, energy in the exhaust, and heat transfer. A heat balance analysis is performed on the engine in order to understand the distribution of energy and exergy flow to improve engine efficiency. Therefore, it is very important to know the fraction of each term which is the aim of the thermal balance experiments. Fu et al. investigated energy and exergy analysis on a naturally aspirated gasoline engine and showed that at low-speed and low-load, cooling fluid mainly contains the waste heat energy while at high-speed and high-load, exhaust gas energy is greater than the cooling fluid energy both in quantity and exergy percentage [1]. For thermal balance analysis, a power generation and heat recovery model was presented by Yan et al. to estimate the efficiency of engines [2]. Ozkan et al. examined the effect of multiple injections on the thermal and exergetic efficiencies on a diesel engine [3]. Their results showed that multiple injections have no significant influence on the thermal efficiency, however, exergetic efficiency decreased. Sezer et al. [4] showed that a lean mixture gives the best first and second law efficiencies by investigating the exergy balance in spark ignition engines. Results also indicated that increasing the initial charge temperature leads to a decrease in the first and second law efficiencies. Rakopoulos and Giakoumis [5] reviewed the first and second laws for all types of engines, by focusing on the main differences between the first and second law analyses. Also, Tsurushima et al. compared the thermal balance for conventional diesel, HCCI and premixed diesel combustion and described the effect of Exhaust Gas Recirculation (EGR). By using EGR, heat losses decreased for both HCCI and premixed diesel combustion at lower load conditions [6].

The paucity of fossil fuels and the pollution problems associated with them have prompted a search for alternative fuels [7]. Therefore, the effects of several alternative fuels on the performance and thermal balance of engines was studied. Costa et al. [8] investigated the energy and exergy analysis in a natural gas/diesel dual-fuel engine. They developed an experimentally validated mathematical model to study the effect of air conditions, the type and quantity of fuel and the exhaustion gases over the engine performance. The effect of hydrogen enrichment on exergy analysis of a lean burn natural gas engine was reported by Ozcan [9]. He showed that by increasing hydrogen fraction, the irreversibility during the combustion decreases, and the second-law efficiency sharply increases close to the lean burn limit. Also, the addition of hydrogen to the fuel and its effect on heat balance in spark ignition engines was studied by Yuksel and Cevis [10]. They showed that adding hydrogen to gasoline

decreases the heat loss to the cooling fluid and unaccounted losses, while the heat loss through the exhaust gases was nearly the same with pure gasoline and thus, engine thermal efficiency improved. Ozcan and Yoylemez studied thermal balance of an LPG fuelled SI engine with the addition of water and it was reported that by increasing the water injection level to the engine, the percentage of output power increased, while the heat transferred to cooling fluid and exhaust gases decreased [11]. Ajav et al. [12] also studied the effect of fuel composition on heat balance in a single cylinder diesel engine operating on diesel, ethanol–diesel blends and fumigated ethanol. It was demonstrated that for more than 15% blending, the thermal balance was significantly different compared to diesel.

Khaliq et al. [13] studied the effect of a turbocharger in a HCCI engine fueled with wet ethanol and demonstrated that the first and second law efficiencies are an increasing function of the turbocharger pressure ratio. Durgun and Sahin [14] developed a multi-zone model to study the heat balance in a turbocharged diesel engine and gasoline fumigation. Results indicated that with an increasing fumigation ratio, thermal efficiency decreases while heat transfer to the walls and exhaust losses increase. The effect of insulated heat transfer surfaces on a diesel engine heat balance was investigated by Taymaz [15] and results pointed out that fuel consumption and heat losses to cooling fluid reduced in the ceramic-coated engine. Also, Giakoumis [16] studied the effect of the isolated cylinder wall on the first and second law in a turbocharged diesel engine. The results revealed that by increasing the load, unlike the first-law, the second-law values were significantly impacted by the insulation. More insulation leads to an increase in the potential for extra work recovery owing to the higher availability content of the exhaust gas. Liu et al. [17] investigated Exhaust gas energy recovery and improvement in engine thermal efficiency. Also, steam turbocharging was developed by Fu et al. [18] as a new approach for exhaust energy recovery in engines. Their study showed that output power and thermal efficiencies can be improved by 7.2% and 2%, respectively, through the use of steam turbocharging.

In this study, the thermal balance of a turbocharged, spark ignition engine fuelled by natural gas was investigated and variation of output power, transferred energy to cooling fluid and exhaust gas energy at different operating conditions were compared experimentally. The effects of turbocharging and fuel type (CNG and gasoline) on thermal efficiency and engine performance were also studied. Finally, based on experimental results, an empirical correlation was suggested to predict the energy of exhaust gases by using exhaust gas temperature and air-fuel ratio which can be measured with the use of sensors.

2. Engine Test Setup

The engine used in this study was a four-cylinder, turbocharged, water cooled, gas spark ignition, which was coupled to an AVL-190kW dynamometer. The engine specifications and operational conditions of the tests are summarized in Table 1. Fig. 2 is a schematic illustration of the experimental test bed.

Fuel consumption was measured using an AVL-735 fuel meter. Analysis of the exhaust gas composition was undertaken using a Horiba-7170D (Gas Analyzer) K-type thermocouples were used to measure the exhaust gas, cooling fluids and intake air temperatures. Table 2 summarizes the accuracy of the measurements and the uncertainty of the results for the tested parameters.

3. Thermal balance calculation

To calculate the thermal balance in the engine, a control volume was assumed around the engine. Figure 2 shows the input and output energies of the control volume.

Based on figure 2, the first law for control volume is as follows:

$$\dot{Q}_f + \dot{Q}_o + \dot{Q}_a = \dot{W}_{sh} + \dot{Q}_e + \dot{Q}_c + \dot{Q}_u \qquad (1)$$

where, $\dot{Q}_f$ is the fuel energy, $\dot{Q}_o$ is the energy caused by burning of consumed oil, $\dot{Q}_a$ is the energy of intake air, $\dot{W}_{sh}$ is the output power on shaft, $\dot{Q}_e$ is the energy of exhaust gases, $\dot{Q}_c$ is the energy which is taken by the cooling fluid of engine and intercooler (cooling energy), and $\dot{Q}_u$ is the unaccounted losses to ambient.

The heat supplied by the fuel was calculated from equation 2:

$$\dot{Q}_f = Q_{LHV,f} \times \dot{m}_f \qquad (2)$$

Where, $Q_{LHV,f}$ is the lower heating value of fuel which is 44.98 MJ/kg.

In the experiment setup, blow-by gases were driven into the combustion chamber and thus, the energy of oil which was burnt should be considered in thermal balance which was shown in equation 3:

$$\dot{Q}_o = Q_{LHV,oil} \times \dot{m}_{oil} \quad (3)$$

Where $\dot{m}_{oil}$ is the amount of burned oil (kg/s) and $Q_{LHV,oil}$ is the lower heating value of oil (33.24 MJ/kg). To determine the burned oil, before and after the tests, the amount of oil was measured and mass flow rate of consumed oil was computed.

The energy of intake air is as follows [19]:

$$\dot{Q}_a = \dot{m}_a(\Delta h_a + w_a \Delta h_{H2O}) \quad (4)$$

Where, $\dot{m}_a$ is the mass flow rate of air (kg/s) which was calculated using the mass flow rate of fuel and air-fuel ratio, Δh_a is the enthalpy difference with standard state (kJ/kg) and $w_a \Delta h_{H2O}$ is the enthalpy increasing due to humidity of air (w_a is the relative humidity).

Energy transferred to the cooling fluid of engine and intercooler was calculated by:

$$\dot{Q}_c = \dot{m}_c \times C_c \times \Delta T_{Engine} + \dot{m}_a \times C_a \times \Delta T_a \quad (5)$$

In equation 5, $\dot{m}_c$ is the mass flow rate of cooling fluid (kg/s), C_c is heat capacity of cooling fluid which is 3.6 kJ/kg.K and ΔT_{Engine} is the temperature difference between inlet and outlet cooling fluid. Energy transferred to the intercooler was determined using the mass flow rate of air over the intercooler and its temperature difference.

The energy of exhaust gases consists of two parts: sensible enthalpy, due to temperature difference between exhaust gases and ambient, and energy in gases because of the incomplete combustion. Since the exhaust is a mixture of gases, the Dalton model was used to compute the sensible enthalpy, and for greater accuracy, the temperature dependent specific heat capacity was also used [19]. Also, incomplete combustion produces carbon monoxide and unburned hydrocarbons which wastes 282995 and 74873 energy (Joules per molecule), respectively [19].

The Mass flow rate of fuel and intake air was measured with flow meters, and by using the global reaction of combustion, the molar flow rate of products in the exhaust gas was computed.

Equation 6 shows the global reaction of fuel combustion and the composition of fuel is given in table 3.

$$\dot{M}_f\left(\frac{mol}{s}\right)\left(C_xH_y + 0.01CO_2 + 0.045N_2\right) + air \rightarrow aCO_2 + bCO + cCH_4 + dH_2O + eO_2 + fNO + gNO_2 + hN_2 + 0.01CO_2 + 0.045N_2 \quad (6)$$

Unaccounted energies consist of heat loss from the engine surface to the surrounds and friction losses in the engine. In this study, this term was computed by the difference between the input energy and the sum of the output work, exhaust gases energy and energy transferred to the cooling fluid and intercooler.

4. Results and discussion

The Thermal balance of the engine operating on gaseous fuel with a turbocharger was established at different loading conditions with a cooling fluid temperature of 90°C and 110°C. Thermal balance was in respect to output power, heat loss through the exhaust gases, heat loss to the cooling and unaccounted losses. The percentages of thermal balance terms at full load with a cooling fluid temperature of 110°C versus engine speed are presented in Figure 3. It can be seen from this figure that as the speed of the engine increased, the percentage of the output power also increased to the maximum amount and then decreased. The percentage of heat loss with exhaust gases increased, which is due to higher exhaust temperature at high speeds. Also, while the engine load and cooling temperature were remaining unchanged, the percentage of coolant heat loss was constant which is consistent with result of Heywood [19]. Besides, by increasing the engine speed, the unaccounted losses decreased, so, at higher engine speed, lower amount of energy will be lost, which shows that the engine attains optimum operation at the later stages.

Data for the Thermal balance and performance parameters are also presented in Tables 4-6. In these tables, output power of engine, exhaust gases energy and transferred energy to the cooling fluid for the four modes of operation are presented.

It can be seen from table 4 that by increasing the temperature of the cooling fluid, thermal efficiency of the engine also increases. This is due to a reduction in the viscosity of the oil and, as a result, friction losses. The maximum thermal efficiency of the engine is 37% and 36.7% for a cooling fluid temperature of 110 °C and 90 °C at full load, respectively. In this table, the effect of load changing on thermal efficiency is considerably. For half load, due to relatively less power taken from the engine, efficiency decreases and more energy is lost due to friction and also pumping losses. The results show that the engine efficiency at full load is 3.08% and 2.98% more than half load, averagely, from 1500 RPM to 5500 RPM when the temperature of the cooling fluid is 90 °C and 110 °C, respectively.

More friction losses at half load are transferred to the cooling fluid. Therefore, the amount of transferred energy to the cooling fluid increases (as shown in Table 5). Also, the results indicate that by increasing the temperature of the cooling fluid, the amount of transferred energy to the cooling fluid decreases. This is due to a lower temperature difference between the engine and cooling fluid.

Results from the experiments point out that the heat transferred to the cooling fluid was 19.5% and 21% for full load at the cooling temperatures of 110 °C and 90 °C respectively, while this ratio increases to 23% and 23.9% at half load.

Table 6 shows the amount and percentage of exhaust gases energy. It can be seen that by increasing the temperature of the cooling fluid, the exhaust gases energy ratio increases which is due to the greater exhaust temperature. Also, by increasing the engine load, the temperature of the exhaust gases rises resulting in an increase in the exhaust gases energy ratio. Based on table 6, the percentage of exhaust gases energy increased averagely by 6% at full load relative to half load and by also increasing the temperature of the cooling fluid from 90 °C to 110°C, the percentage of exhaust gases energy increased 3% averagely.

The NOx and HC emission levels is presented in figure 4 for half and full loads and also the different cooling temperatures. Due to throttling in half load, internal EGR offers significant potential for reducing the NOx emission. Also, by increasing the cooling temperature, the engine operates at a warmer temperature, and as result, the maximum in-cylinder temperature increases resulting in more NOx emissions produced. Due to a more incomplete combustion relative to full load, in part load operation, more HC was produced. Increasing incomplete combustion leads to a decrease in the exhaust gas temperature and as a result, percentage of exhaust gases energy is decreased in part load operation.

4.1. Comparing the NA and TC engines performance

The effect of turbo charging on the engine's thermal efficiency and output power is shown in Figure 5. It can be seen that by adding the turbocharger, the power and thermal efficiency of the engine increases. Assuming a control volume around the turbine of the turbocharger and intercooler, at an engine speed of 5500 RPM, 16.3 kW of the exhaust gases energy was returned into the control volume by the turbine while 11.6 kW was lost through the intercooler (as shown in Figure 6). This leads to a 1.4% increase in the thermal efficiency. The turbocharger also

causes an increase in the pressure of the intake air, and therefore, an increase in the maximum and mean effective pressure of the engine. In the turbocharged engine, thermal efficiency increased 3.4% toward the natural aspirated engine at 5500 RPM. It can also be seen from figure 5 that the maximum increase in thermal efficiency for the TC engine was 4% at around 2500 RPM.

To understand the details of the operation of a thermal system and also the locations, causes and magnitudes of energy resource waste in the system, an exergy analysis of the system could be helpful. The exergy rate balance for the engine operating at a steady state can be expressed as:

$$X_{fuel} + X_{in} - X_W - X_{ex} + \sum\left(1 - \frac{T_0}{T_j}\right) Q_c - X_{dest} = 0 \qquad (7)$$

where X_{fuel} , X_W and X_{ex} are the exergies of the fuel, brake power and exhaust gas, respectively and X_{in} is the exergy transfer through intake process . The term $\sum\left(1 - \frac{T_0}{T_j}\right) Q_c$ indicates the exergy transfer by the heat where Tj is the absolute temperature of the boundary section from where the heat is rejected. Inserting the values for these parameters into Equation (7), the exergy destroyed in the engine (X_{dest}) can be evaluated. The details of the computations can be found in literatures [20, 21].

Exergy distribution at full load and a cooling fluid temperature of 90°C are shown in figure 7. In this figure, the flow exergy is the transferred exergy through intake and exhaust process. The exergetic efficiency of the engine is calculated by the ratio of the brake power to the fuel exergy input:

$$\varepsilon = \frac{X_W}{X_{fuel}} \qquad (8)$$

Where ε is the exergetic efficiency (second law efficiency) and X_W is equal to output power. In figure 8, the second law efficiency of TC and NA engines is compared. The exergetic efficiencies of the engine follows similar trends with the thermal efficiency (figure 5), however, the exergetic efficiency is 3.2% lower than the thermal efficiency (TC engine) averagely, this is because a higher amount of fuel exergy is supplied to the engine compared to the fuel energy. Also, comparing the exergetic efficiency of TC and NA engines indicates that using the unused output exergy in exhaust gases can increase output power and therefore improve engine efficiency. Based on figure 8, second law efficiency of TC engine is 3.6% higher than NA engine, averagely.

4.2 The effect of fuel type on performance of engine

The effect of fuel type on thermal balance also was investigated using both natural gas and gasoline to fuel the engine. For gaseous fuel, MBT spark timing was used for all operation conditions, while in gasoline mode, to avoid knock, the spark timing was retarded. Results showed that when the engine is fuelled by gasoline, the output power is greater than it is for gaseous fuel. However, thermal efficiency of the engine is higher for natural gas than it is for gasoline, as illustrated in figure 9. This is due to the decrease in volumetric efficiency and less air entering the cylinder resulting in decreased power for the gaseous fuelled engine. On the other hand, the heat values of natural gas and gasoline are 45 MJ/kg and 42.75 MJ/kg respectively, which are caused by more thermal efficiency in the gas engine. Also, in gas engine, because of higher octane number of natural gas, advanced spark timing was used which leads to improve the thermal efficiency. Figure 9 shows that the maximum power of the gasoline engine at 5500 RPM was 5.5kW more than the gas engine while the maximum thermal efficiency of the gas engine at 2500 RPM was 4.5% more than the gasoline engine.

In figure 10, NOx, HC and CO emissions of CNG and gasoline engines are shown. According to part (a) of figure 10, gaseous fuel results in more NOx emissions. It should be noticed that NOx formation takes place at high temperatures and the increase of NOx is caused by the higher combustion temperature of natural gas. For gaseous fuel there is no cooling effect which will cause a higher initial temperature for in-cylinder charge and more spark advance is also needed because of the low flame speed of CNG which rises peak of combustion temperature and pressure. Based on Parts (b) and (c) of figure 10, gaseous fuel produces lower HC and CO emissions. CO and HC concentration in exhaust gases mostly depends on air/fuel ratio and a rich mixture (gasoline engine at full load) causes more CO and HC in exhaust gases [19]. Carbon to hydrogen ratio of fuel (C/H ratio) is another parameter which affects the formation of CO and as a result, use of natural gas causes lower CO emissions.

4.3 The empirical equation for exhaust gases energy

Thermal balance tests are lengthy and costly processes as they require great care and attention, thus finding the general mathematical relations would help predicting the heat balance for different operation conditions. So, the experimental data was used to find an empirical correlation to predict the energy of exhaust gases. Two main parameters are selected to characterize $\dot{Q}_e$: exhaust gas temperature and air-fuel ratio. Air-fuel ratio and temperature can be simpler to measure than exhaust gas compositions through the use of sensors. The correlation that was found to work well for the experimental data is:

$$\dot{Q}_e = (A + B_1 T + B_2 T^2) \quad (9)$$

Where:

$$A = 8388.5 - 13744.4\lambda + 5165.9\lambda^2$$

$$B_1 = 1.3 - 0.6\lambda + 0.22\lambda^2$$

$$B_2 = 0.00002 - 0.00007\lambda + 0.00005\lambda^2$$

In this equation, λ is the air-fuel equivalence ratio and T is the temperature of the exhaust gases.

The predicted exhaust gas energy using the empirical equation and experimental data was compared in figure 11 for full and half loads with a cooling temperature of 90 °C.

The results indicated that the correlation captures the trend of $\dot{Q}_e$ variations, showing good agreement with the experimental data for the majority of operating conditions. The standard deviation and uncertainty of predicted results for the empirical correlation for all operating conditions are shown in table 7.

The maximum uncertainty of 12.8 kW was found in the predictions from equation (9) for the full load operating condition and the cooling temperature of 110 °C. The uncertainty is determined by 2σ, where σ is the standard deviation of residual errors. This means that the true value, with 95 percent confidence, lies within ±2σ of the estimated value [22].

5. Conclusion

In this study the thermal balance of a turbocharged SI engine operating on natural gas was investigated experimentally. From the results of this study, the following conclusions can be deduced:

1- By increasing cooling fluid temperature from 90 °C to 110°C, the maximum thermal efficiency of the engine increased 0.3%, the average ratio of the heat loss to the cooling fluid decreased 2.5% and the ratio of exhaust gas energy increased 3%.

2- Thermal efficiency and the ratio of exhaust gas energy for full load was, on average, 3.03% and 6% more than for half load while the average ratio of heat loss to the cooling fluid for full load was 3.2% less than half load.

3- The maximum thermal efficiency of the turbocharged engine was 4% more than natural aspirated at 2500 RPM. Also, the maximum thermal efficiency of the gas engine at 2500 RPM was 4.5% more than gasoline engine.

Therefore, by using the turbocharger and natural gas as fuel in the engine, thermal efficiency of the engine increased 8.5%.

4- By using the turbocharger, a part of wasted energy in exhaust gases can be converted to useful power and therefore improve exergetic efficiency. Based on results, second law efficiency of TC engine is 3.6% higher than NA engine, averagely.

5- An empirical correlation was suggested to predict the energy of the exhaust gases using exhaust gas temperature and the air-fuel ratio. The correlation showed good agreement with the experimental results for the majority of operating conditions. The maximum standard deviation and uncertainty of 6.4 and 12.8 kW was found in the predications from the correlation.

References

[1] J. Fu, J. Liu, R. Feng, Y.Y. Wang, Y. Wang, Energy and exergy analysis on gasoline engine based on mapping characteristics experiment, Appl. Energ. 102(2013) 622–630.

[2] K.T. Yun, H. Cho, R. Luck, P.J.Mago, Modeling of reciprocating internal combustion engines for power generation and heat recovery, Appl. Energ. 102 (2013) 327–335.

[3] M. Ozkan, D.B. Ozkan, O. Ozener, H.Yilmaz, Experimental Study on Energy and Exergy Analyses of a Diesel Engine Performed with Multiple Injection Strategies: Effect of Pre-Injection Timing, Appl. Therm. Eng. 53 (2013) 21-30.

[4] I. Sezer, A. Bilgin, Effects of charge properties on exergy balance in spark ignition engines, Fuel. (2012) Available online 17 October 2012.

[5] C.D. Rakopoulos, E.G. Giakoumis, Second-law analyses applied to internal combustion engines operation, Prog. Energ. Comb. Sci. 32(2006) 2–47.

[6] T. Tsurushima, A. Harada, Y. Iwashiro, Y. Enomoto, Y. Asaumi, Y.Aoyagi, Thermodynamic Characteristics of Premixed Compression Ignition Combustions, SAE paper 2001-01-1891; 2001.

[7] T. F. Yusaf, D.R. Buttsworth, K. N. Saleh , B.F. Yousif, CNG-diesel engine performance and exhaust emission analysis with the aid of artificial neural network, Appl. Energ. 87 (5) (2010) 0306-2619.

[8] Y. Costa, A. Lima, C. Filho, L. Lima, Energetic and exergetic analyses of a dual-fuel diesel engine, Renew. Sust. Energ. Rev.16 (2012) 4651–4660.

[9] H.Ozcan, Hydrogen enrichment effects on the second law analysis of a lean burn natural gas engine, Int. J. Hydrogen Energ. 35(2010)1443–1452.

[10] F. Yuksel, M.A. Ceviz, Thermal balance of a four stroke SI engine operating on hydrogen as a supplementary fuel, Energy. 28 (2003)1069–1080.

[11] O. Hakan M.S. Söylemez, Thermal balance of a LPG fuelled, four stroke SI engine with water addition. Energ. Convers. Manage. 47 (2006) 570–581.

[12] E.A. Ajav, T.K. Singh, Thermal balance of a single cylinder diesel engine operating on alternative fuels, Energ. Convers. Manage. 41 (2000)1533–1541.

[13] A. Khaliq, S. K. Trivedi, I. Dincer, Investigation of a wet ethanol operated HCCI engine based on first and second law analyses, Appl. Therm. Eng. 31 (2011)1621–1629.

[14] O. Durgun, Z. Şahin, Theoretical investigation of heat balance in direct injection (DI) diesel engines for neat diesel fuel and gasoline fumigation, Energ. Convers. Manage. 50 (2009) 43–51.

[15] I. Taymaz, An experimental study of energy balance in low heat rejection diesel engine, Energy. 31 (2006) 364–371.

[16] E.G. Giakoumis, Cylinder wall insulation effects on the first- and second-law balances of a turbocharged diesel engine operating under transient load conditions, Energ. Convers. Manage. 48 (2007) 2925–2933.

[17] J.P. Liu, J.Q. Fu, C.Q. Ren, L.J. Wang, Z.X. Xu, B.L.Deng, Comparison and analysis of engine exhaust gas energy recovery potential through various bottom cycles, Appl. Therm. Eng. 50(2013) 1219–1234.

[18] J. Fu, J. Liu, Y. Yang, C. Ren, G. Zhu, A new approach for exhaust energy recovery of internal combustion engine: Steam turbocharging, Appl. Therm. Eng. 52 (2013)150–159.

[19] J.B. Heywood, Internal combustion engines fundamentals, McGraw Hill Book Company, New York, 1989.

[20] J. Zheng, J.A. Caton, Second law analysis of a low temperature combustion diesel engine: Effect of injection timing and exhaust gas recirculation, Energy. 38 (2012) 78-84.

[21] C. Sayin, M. Hosoz , M. Canakci, I. Kilicaslan, Energy and exergy analyses of a gasoline engine, Int. J. Energy Res. 31(3) (2007) 259–273.

[22] R. J. Moffat, Describing the uncertainties in experimental results. Exp. Therm. Fluid Sci. 1 (1988) 3–17.

Nomenclature

$\dot{m}_a$ air mass flow (kg/s)

$\dot{m}_c$ mass flow rate of cooling fluid (kg/s)

$\dot{m}_f$ fuel mass flow (kg/s)

$\dot{m}_{oil}$ oil mass flow (kg/s)

T absolute temperature (K)

w_a relative air humidity

σ standard deviation

Abbreviations

AFR air-fuel ratio

CNG compressed natural gas

DI direct injection

EGR exhaust gas recirculation

HCCI homogeneous charge compression ignition

LPG liquefied petroleum gas

MBT maximum brake torque

NA naturally aspirated

RPM revolution per minute

TC turbo charger

VVT variable valve timing

List of Tables

1 Engine specifications

2 Accuracy of measurements and uncertainty of computed results

3 The fuel composition

4 Output power and thermal efficiency of engine

5 Energy transferred to the cooling fluid and intercooler (cooling energy)

6 Energy of exhaust gases

7 Standard deviation and uncertainty of empirical correlation results

List of Figures

1 Schematic of Engine test bed

2 Control volume around the engine

3 Thermal balance at full load and 110°C cooling water temperature

4 The effect of engine operation condition on NOx and HC emissions

5 Comparing of the power and thermal efficiency in turbocharged and naturally aspirated engines

6 The recovered energy by turbocharger and intercooler

7 Exergy distribution at full load and cooling fluid temperature of 90 C

8 Exergetic efficiency of TC and NA engines

9 Comparing of the power and thermal efficiency in gasoline and gas engines

10 Comparing of (a) NOx, (b) HC and (c) CO emissions in gasoline and gas engines

11 Comparison of experimental results and the equation 7 at full and half loads with cooling temperature of 90°C

Tables

Table 1: Engine specifications

Parameter	Value (units)
Displacement	1.7L
Fuel	Natural Gas
Bore	78.6 mm
Stroke	85mm
Number of cylinder	4
Number of valves	4
Maximum Torque@2200RPM	215N.m
Maximum power@ 5500RPM	110kW
Compression Ratio	9.8:1
Valve opening mechanism	VVT

Table 2: Accuracy of measurements and uncertainty of computed results

Measurements	**Accuracy**
λ sensor	±0.001
NO_x	±5ppm
CO	±3ppm
HC	±1ppm
Speed	±2rpm
Torque	±0.1Nm
Temperature	1℃
Computed results	Uncertainty (%)
Fuel volumetric rate	±1
Cooling fluid volumetric rate	±0.1
Power	±1

Table 3: The fuel composition

Species	Volume ratio
CH_4	0.881
C_2H_6	0.047
C_3H_8	0.0102
C_4H_{10}	0.0047
C_5H_{12}	0.0017
C_6H_{14}	0.0004
CO_2	0.01
N_2	0.045

Table 4: Output power and thermal efficiency of engine

Engine Speed	Full Load 110°C		Half Load 110°C		Full Load 90°C		Half Load 90°C	
(RPM)	$\dot{W}_{sh}$(kW)	η_{th}(%)	$\dot{W}_{sh}$(kW)	η_{th}(%)	$\dot{W}_{sh}$(kW)	η_{th}(%)	$\dot{W}_{sh}$(kW)	η_{th}(%)
1500	17.1	34.7	8.2	31.3	16.6	34.5	8.2	31.2
2000	29.7	36	15.1	32.9	30.2	36.1	14.9	33
2500	55.9	37	27.8	34.5	56.1	36.7	28.1	34.2
3000	67.5	36.8	33.1	34.1	67.4	36.5	33.2	33.7
3500	78.8	36	39.2	33.2	78.6	35.6	39.1	33
4000	89.8	35.3	44.8	32.6	90.1	35.1	44.4	32
4500	101.1	34.8	50.4	31.4	101.1	34.5	50.5	31.6
5000	108.2	33.8	54	30.8	106.9	33.5	53.7	30.5
5500	110.4	32.6	55.3	29.4	110.5	32.4	55	29.1

Table 5: Energy transferred to the cooling fluid and intercooler (cooling energy)

Engine Speed (RPM)	Full Load 110°C		Half Load 110°C		Full Load 90°C		Half Load 90°C	
	$\dot{Q}_c$(kW)	$\dot{Q}_c$(%)	$\dot{Q}_c$kW)	$\dot{Q}_c$(%)	$\dot{Q}_c$(kW)	$\dot{Q}_c$(%)	$\dot{Q}_c$(kW)	$\dot{Q}_c$(%)
1500	11.8	24	7.7	29.2	9.5	20.4	6	23.1
2000	15	18.2	12.6	27.6	17.3	20.6	11.2	24.9
2500	30.6	20.3	17.5	21.7	34.1	22.3	20.6	25
3000	33.9	18.4	23	23.7	40.3	21.8	24.1	24.5
3500	39.8	18.2	27.9	23.6	44.8	20.3	26.8	22.6
4000	44.5	17.5	29.6	21.5	53.1	20.7	33.1	23.8
4500	55.9	19.2	36.2	22.5	61.9	21.1	36.3	22.7
5000	63.5	19.7	39	22.2	66.6	20.9	41.9	23.8
5500	67.9	19.9	43.3	23	70.7	20.7	44.3	23.5

Table 6: Energy of exhaust gases

Engine Speed (RPM)	Full Load 110°C		Half Load 110°C		Full Load 90°C		Half Load 90°C	
	$\dot{Q}_e$(kW)	$\dot{Q}_e$(%)	$\dot{Q}_e$(kW)	$\dot{Q}_e$(%)	$\dot{Q}_e$(kW)	$\dot{Q}_e$(%)	$\dot{Q}_e$(kW)	$\dot{Q}_e$(%)
1500	15	30.5	6	22.6	10.5	23.8	6.2	22.6
2000	28.2	34.1	11.7	26.6	22.3	29	13.1	25.5
2500	59.4	39.3	24.1	30.5	46.4	33.7	27.7	29.9
3000	75.5	41.4	31.2	32.1	59.1	35.9	35.4	32
3500	96.8	44.2	40.5	34.3	75.6	38.6	45.7	34.2
4000	115.8	45.5	50	36.6	90.6	40.3	55.9	35.3
4500	133.2	45.8	59.4	37	105.2	41.4	66.2	35.9
5000	149.6	46.8	66	37.6	117.7	42.5	74.7	36.9
5500	161.3	47.3	72.7	38.7	127.6	43.8	82.8	37.4

Table 7: Standard deviation and uncertainty of empirical correlation results

Operating Condition	Standard Deviation (σ)	Uncertainty (2σ)	Percentage of Uncertainty
Full load, 90°C	5 kW	10 kW	6.5%
Half load, 90°C	4.4 kW	8.8 kW	10%
Full load, 110°C	6.4 kW	12.8 kW	7.9%
Half load, 110°C	2.6 kW	5.2 kW	6%

Figures

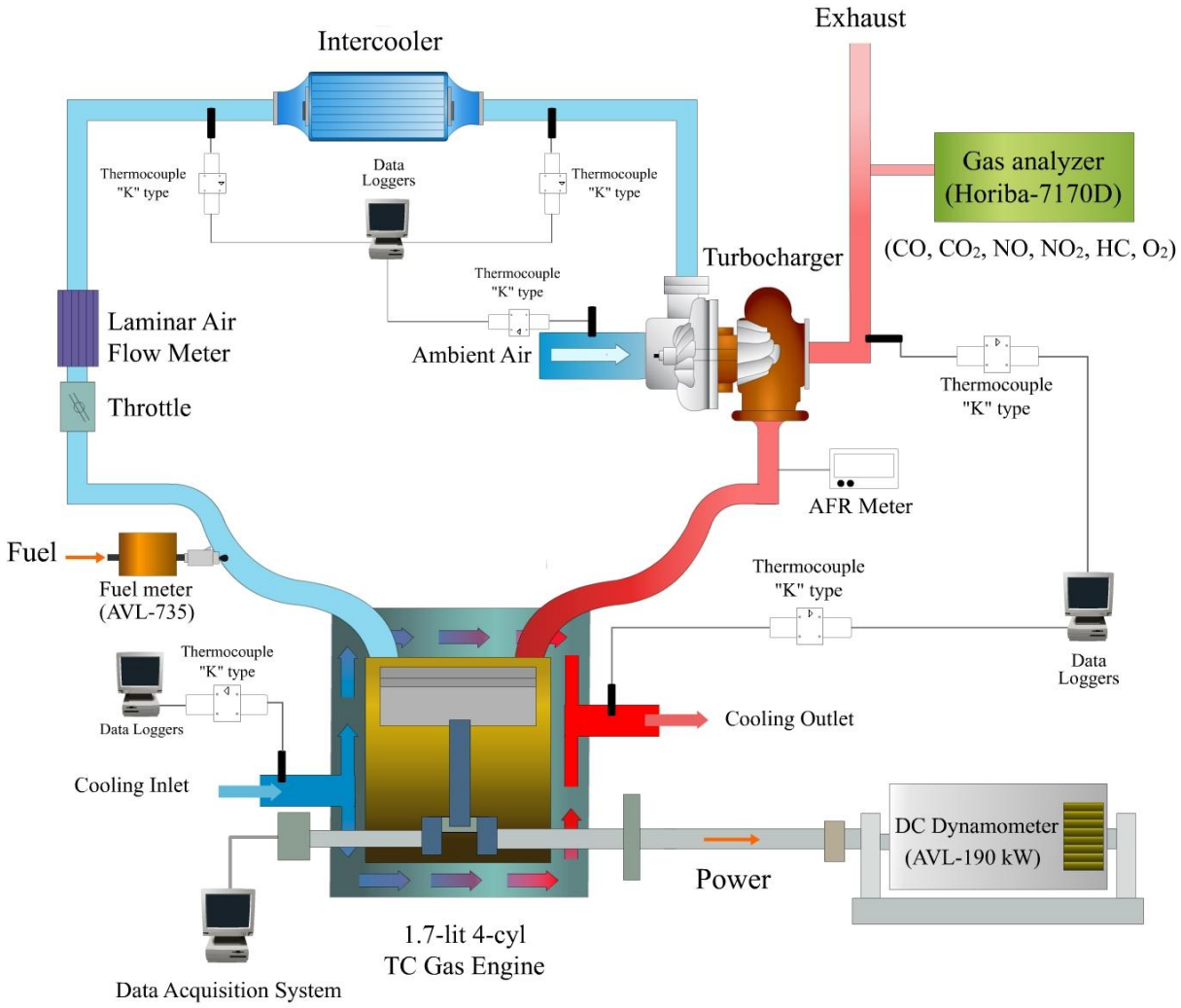

Fig. 1 Schematic of Engine test bed

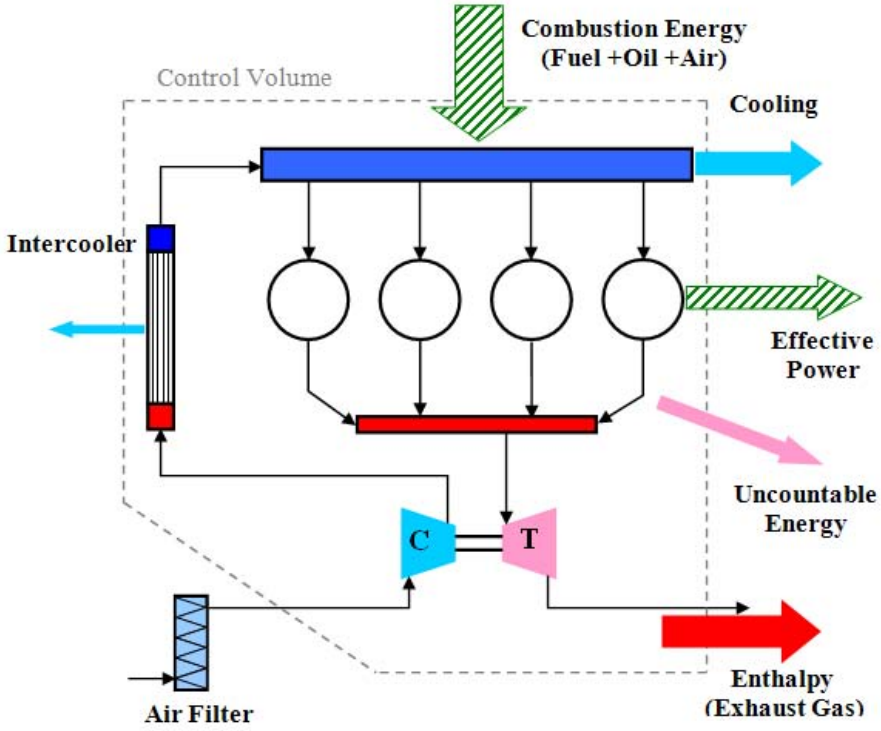

Fig. 2 Control volume around the engine